

Automated analysis of septal fluorescence peak intensity

Abstract

Analysis of peptidoglycan and bacterial cell wall by fluorescence microscopy can teach us a lot about the cell growth dynamics and cell morphogenesis. Analysis of these images manually is time consuming. In this work, we present the comparison between manual data collection of fluorescence intensity for the dyes FM 4-64, Nile Red (which both stain membranes, accumulating more in fluid membrane regions) and HADA (which is incorporated into newly synthesized peptidoglycan, marking peptidoglycan synthesis activity) in *Bacillus subtilis* and a more automated method of data collection based on the ChainTracer plugin for FIJI. We also present an additional tool created on this software which allows the user to measure fluorescence profiles along the short axis (width) of the cell. Our data shows that for individual measurements the automatically collected data matches the manually collected data. Our data shows evidence of colocalization between HADA and FM 464 dyes, and between HADA and Nile Red, which suggests that new peptidoglycan synthesis is happening in the same place as septa formation.

Introduction

As microbe imaging techniques have progressed, it has become cheaper and faster to produce large datasets of images. The large amount of data provides researchers with more possibilities of statistical analysis of single celled organisms. The process of manually analysing these images has become a problem as the sheer number of images has kept increasing. Manual analysis of large datasets is prone to mistakes as researchers will inevitably make errors when repeating the same menial task many times over. On top of this, the process of analysing many images is extremely time consuming for researchers. Many different tools have been developed in order to make image analysis faster and more automated. For example, ChainTracer has been developed for septa determination for species which grow in chains (Syvertsson, Vischer, Gao, & Hamoen, 2016). MicrobeJ has been developed for high throughput analysis of cells and fluorescence localization (Ducret, Quardokus, & Brun, 2016). SuperSegger is a tool for image segmentation and cell fluorescence and morphology determination (Stylianidou, Brennan, Nissen, Kuwada, & Wiggins, 2016).

Cell elongation and division are topics of main interest that are explored using large sets of microscopy images. These processes are correlated with the assembly of different structures on the cytoplasmic membrane of bacteria. Some of the most popular structures that are studied are elongasomes, and divisomes. Divisomes are responsible for cell constriction and new peptidoglycan synthesis during division. Elongasomes are modified versions of the divisome. Elongasomes lack the constricting function and are responsible for cell elongation, having peptidoglycan synthesis as one of the main functions. (Typas et al., 2012; Zhao et al., 2017). Our group is interested in a pair of proteins called flotillins (FloA and FloT), that are associated with the organization of functional membrane microdomains (FMMs) (García-Fernández et al., 2017).

Recently, our group analyzed the function of flotillins in peptidoglycan synthesis in *Bacillus subtilis* species. This work was done by the observation of wild-type *Bacillus subtilis* cells, and a mutant that has the genes *floA* (*yqfA*) and *floT* (*yuaG*) knocked out ($\Delta floAT$). Cells were stained with different lipid stains which bind to lipid membranes, binding slightly stronger to more fluid membrane regions (Nile Red, FM 464) and a D-alanine analogue (HADA) that tags sites with active peptidoglycan synthesis, and imaged on a fluorescence microscope (Zielińska et al., 2020).

Bacillus subtilis is a bacterial species that tends to grow in long chains of attached cells which cannot be distinguished easily when observed using phase contrast microscopy. The septum is a good indicator of where one cell ends, and another starts. The septum contains lipids which can be made visible using fluorescent dyes (Syvertsson et al., 2016). The septal membrane is more fluid than the regular cell membrane, allowing the septa to present higher fluorescence intensity under a fluorescence microscope. ChainTracer is a project which utilizes the ObjectJ plugin for Fiji in order to automatically divide chains in individual cells by measuring fluorescence peaks along the cell chain. ChainTracer makes it possible to automatically measure cell length and width of cells in a chain. (Syvertsson et al., 2016)

ChainTracer is a program which identifies fluorescence profiles in microscopy images that are similar to septa formation, and uses it to identify individual cells. This tool can also be used to determine fluorescence localization along the length of a chain of cells. When analysing the fluorescence intensity along the cell it is not yet possible to determine if the fluorescent dyes are more concentrated in a specific region of the cell in comparison to another. At the same time, there is no data of the background fluorescence, which is a challenge for making definitive statements on the intensity of fluorescence on cell structures.

The microscopy images used in this work, and the manual measurements had been previously collected (Zielińska et al., 2020). In this work we explored the possibilities of using ChainTracer for collecting fluorescence peak intensity values and its location within the cell, so it can be compared to the previously manually collected data (Zielińska et al., 2020). This was done using an existing tool in ChainTracer which measures fluorescence along the long axis of the cell. Additionally we developed a new tool for measuring fluorescence along the short axis (width) of the cell.

Methodology

Cell Growth and acquisition of images used in this study

All images used in this analyses were acquired previously by other members of the group according to the procedures described in Zielińska et al., 2020.

Two strains of *Bacillus subtilis* cells were used, a wild-type (WT), and a double knockout mutant for genes *yqfA* and *yuaG* ($\Delta floAT$). Both strains were grown in LB media, and incubated at 37°C until they reached exponential growth phase. Once in this growth phase, cells were recovered, stained and observed under the fluorescence microscope as described in Zielińska et al., 2020.

Image analysis

For image analysis FIJI was used in combination with the ChainTracer plugin. The ChainTracer function for finding fluorescence profiles along the long axis (length) of the cell was used for finding the peak intensities.

Statistical analysis

The program Graphpad Prism was used to perform the statistical analysis of the data generated in this work. The same statistical treatment used on Zielińska et al., 2020 was performed in our data. A non-parametrical Mann-Whitney test was done comparing the results obtained for the fluorescence peak intensity in WT cells and $\Delta floAT$ mutants using approximately 140 cells in each analysis.

Development of the tool

The new tool in ChainTracer allowing fluorescence measurement along the width of the cell is based on the previously existing tool to measure fluorescence along the cell length. The previously existing tool works in the StraightCells image created by ChainTracer. In the StraightCells image all cells are displayed in a straight horizontal position inside a box (Figure 1a).

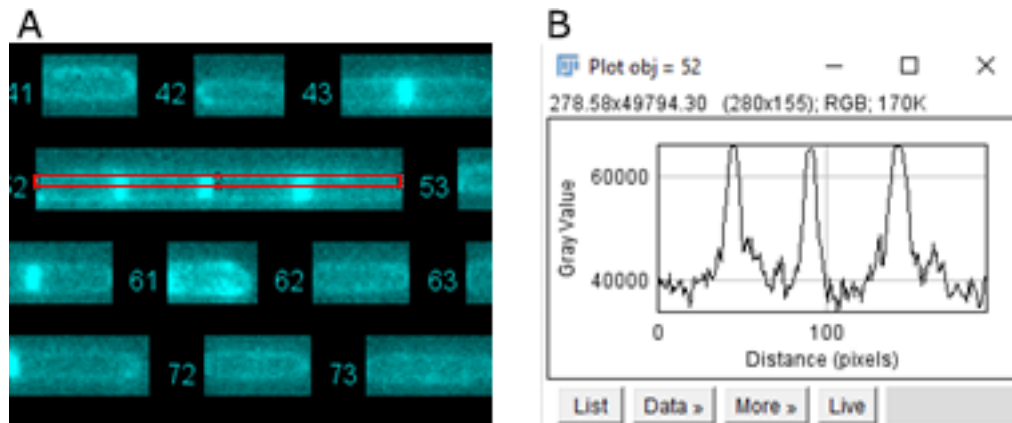


Figure 1 The ChainTracer tool for measuring fluorescence along the long axis of the cell. A) StraightCells image generated by the program. B) Fluorescence profile along the red box drawn through the length of a cell chain in the panel A.

The tool measuring the fluorescence along the cell length creates a rectangle in middle of the cell box (red rectangle in figure 1a) and creates a fluorescence profile along the length of the rectangle (Figure 1b). This works because the cell box is made around the cell chain (Figure 1a). A tool for measuring fluorescence across the width of the cell cannot work this way as in some cell chains a septum is exactly in the middle of the cell box. In this case, the result would be a graph of the fluorescence across the septum, and not across the cell cytoplasm. That is why the x coordinate (were the vertical rectangle should be drawn) for the position of the rectangle along the short axis of the cell (red rectangle in figure 2a) is based on the cursor location instead of the middle of the cell chain box. This way the user can decide whether to produce a graph for the septal fluorescence intensity or for the cytoplasm fluorescence intensity (Figure 2b).

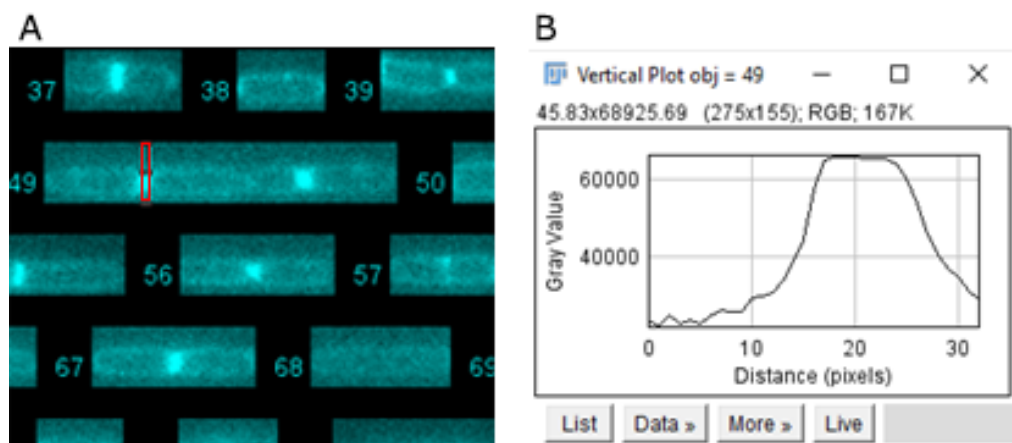


Figure 2 The ChainTracer tool for measuring fluorescence along the short axis of the cell A) StraightCells image generated by the program. B) Fluorescence profile along the red box drawn through the width of a cell chain.

The fluorescence peaks of the cells were found automatically using the tool for measuring fluorescence along the cell chain length described above. The septal fluorescence was compared to the background fluorescence inside the cell. The comparison to the cell background was done by taking the median value of the fluorescence profile and subtracting this value from the peak value

Results

1. Comparison between automatically and manually fluorescence intensity measurement

HADA

In order to test whether collected data via the more automated ChainTracer approach is reliable, a comparison was done between the data collected through the method developed in this work, and the data collected manually in a previous work of our group (Zielińska et al., 2020). If both methods of collecting data from the same images give a similar dataset this would imply that the automatic data collection is reliable. The final value of fluorescence intensity for each cell was determined as described in the method.

The HADA fluorescence peak values collected automatically (Figure 3) are lower than the data collected manually (WT (auto) C mean = 784,2 compared to WT (manual) mean = 1350. $\Delta floAT$ (auto) C mean = 872,9 compared to $\Delta floAT$ (manual) mean = 1401). Even though the values are in the same range, there is a large discrepancy between the two datasets. A possible explanation for this discrepancy is that handpicked septa might show higher fluorescence as there might be a tendency to pick clearly visible septa more often than picking septa with relatively low fluorescence.

For both datasets, the one collected manually and the one collected automatically, the values for WT and $\Delta floAT$ peaks were statistically different. The difference between the WT and $\Delta floAT$ peak values is smaller in the automatically collected data (Hodges-Lehmann difference = 79,71) than in the manual data (Hodges-Lehmann difference = 172,2)

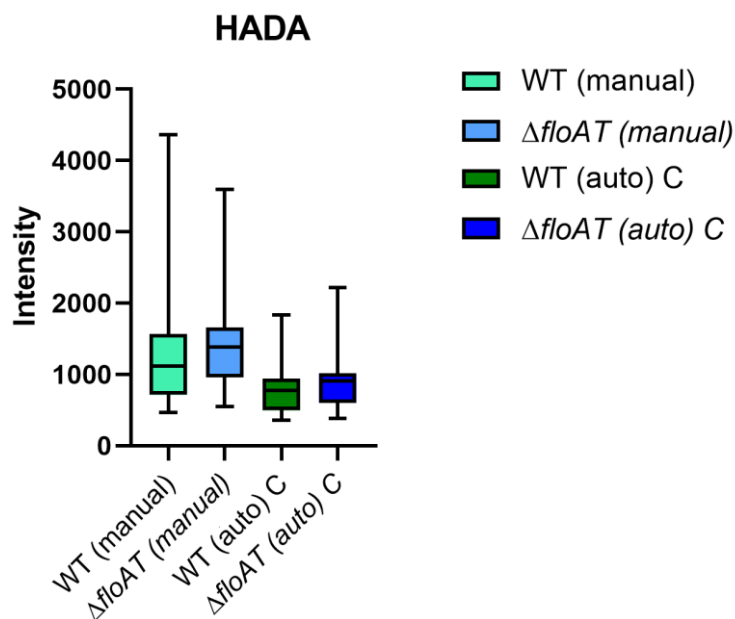


Figure 3 Peak fluorescence intensity of HADA along cell length. 140 cells were used on the manual analysis, and 270 on the automated analysis.

Nile Red

The Nile Red measurements (Figure 4) using the automated method also show a lower value than the manual method for both $\Delta floAT$ and wild type cells just as presented in the HADA measurements (WT (auto) C mean = 6804 compared to WT (manual) mean = 8605. $\Delta floAT$ (auto) C mean = 6900 compared to $\Delta floAT$ (manual) mean = 11436). There is a difference between the $\Delta floAT$ peak data and the wild type peak data in the automatically collected dataset but it is not statistically significant. The difference between the $\Delta floAT$ and wild type peaks is statistically significant in the dataset collected manually.

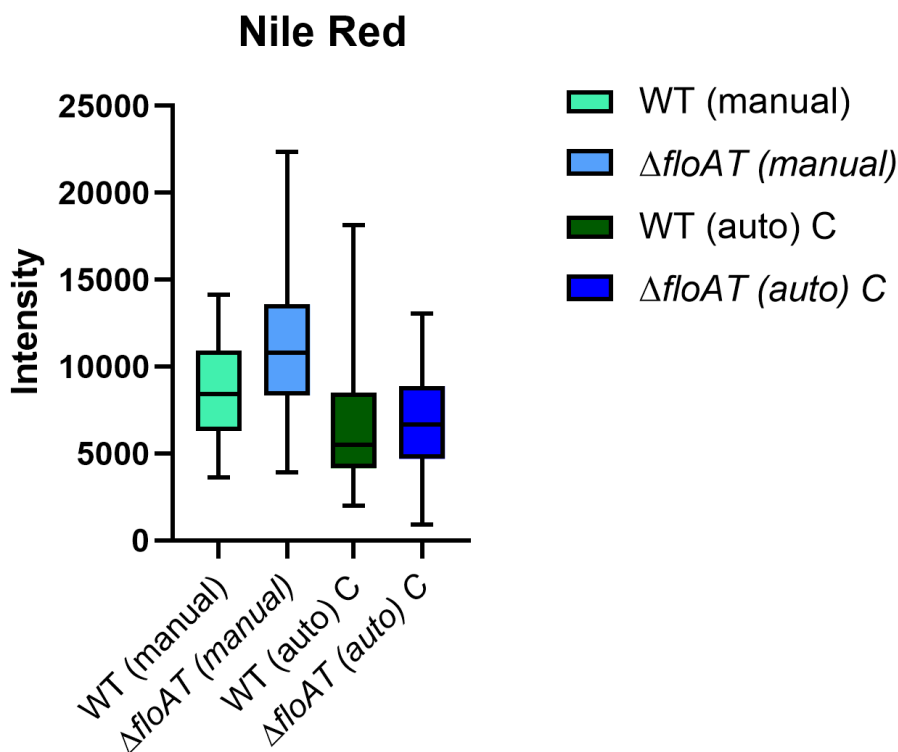


Figure 4 peak fluorescence of Nile Red along cell length. 140 cells were used on the manual analysis, and 134 on the automated analysis.

FM 464

The FM fluorescence peaks measured automatically are considerably lower than the ones measured manually (WT (auto) C mean = 343,4 compared to WT (manual) mean = 490,2. $\Delta floAT$ (auto) C mean = 359,7 compared to $\Delta floAT$ (manual) mean = 597,5) (Figure 5). The difference between the $\Delta floAT$ and wild type measurements are not statistically significant in the automatically collected data. This is in contrast with the data collected manually where the differences between these populations are statistically significant.

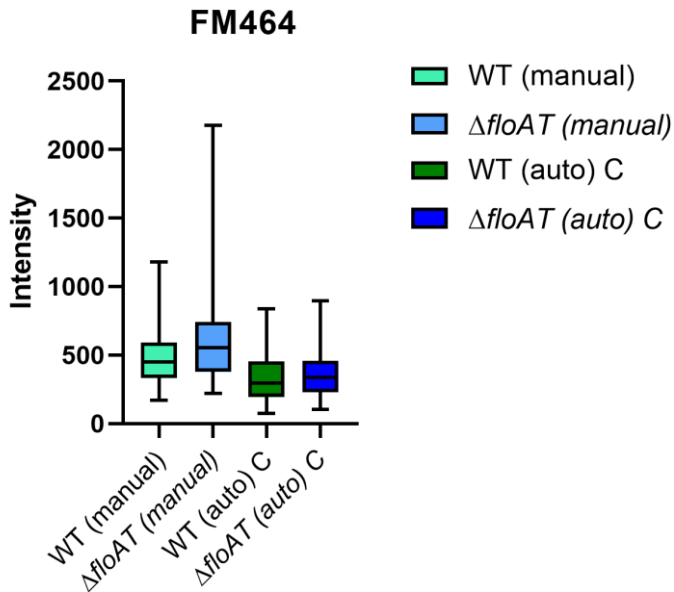


Figure 5. Median fluorescence intensity of FM 464 along cell length. 140 cells were used on the manual analysis, and 154 on the automated analysis.

2. Using the median fluorescence value as cell background fluorescence

In order to check if the median value of the fluorescence profile through the entire cell along the long axis is a good measure of the background fluorescence in a cell, we measured the fluorescence inside the cell. We manually selected a value from the region representing the cytoplasm (Figure 6) and compared this to the median value of the fluorescence profile of the entire chain of cells found using the ChainTracer tool. This was done for 5 cells of each dataset (WT HADA, MT HADA, WT FM, MT FM, WT NR, MT NR).

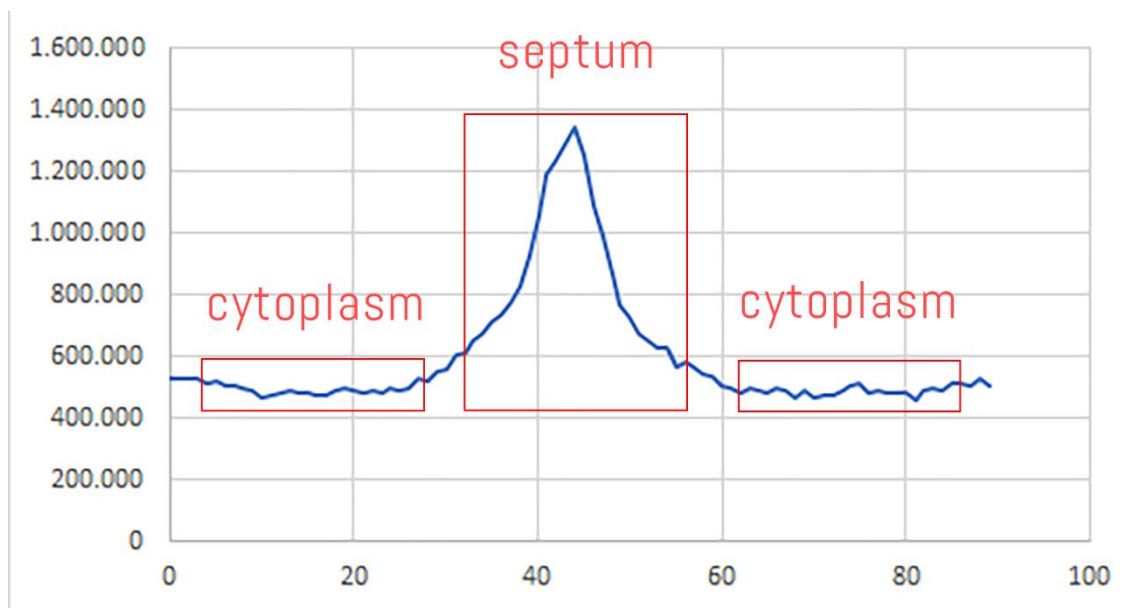


Figure 6 Fluorescence profile through the chain length of a cell with a single septum

On average the median value deviated 2.3% from the manually collected value. In comparison, the intensity of fluorescence in different regions of the cell cytoplasm, fluctuates by far more than 2.3%.

The highest deviation of the median from the manual data found was 10%. This a large deviation and could suggest that this method might be unreliable, but this deviation was found in a cell which had extreme fluorescence fluctuation inside the cytoplasm (Figure 7). This fluctuation is not normally present in cells. In this case, the fluorescence profile in cell cytoplasm presents a difference of 20% between the lowest and the highest point.

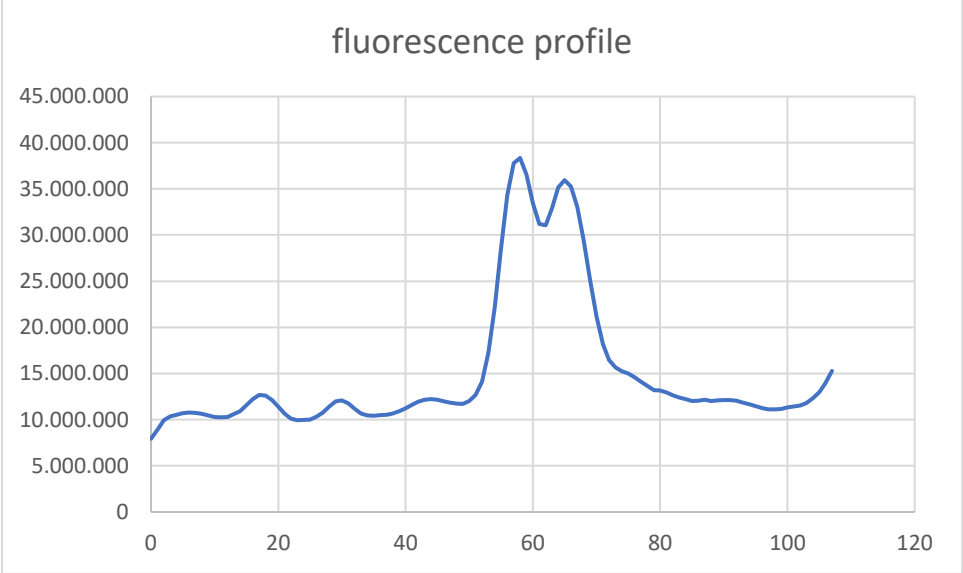


Figure 7 fluorescence fluctuation in the cytoplasm of a cell

Disregarding this datapoint the highest deviation the median fluorescence value had from the manually found value was less than 5% and the average deviation drops to 2%. This shows that using the median of the cell fluorescence profile is a reliable way of finding the cell background fluorescence.

3. Comparing measurements of fluorescence along the cell length

In order to check whether the difference in datasets was due to the different measuring methods, the fluorescence of each cells was measured along its length using the automated method and manually. This was done for FM464, NR and HADA dyes in both WT and $\Delta floAT$ cells.

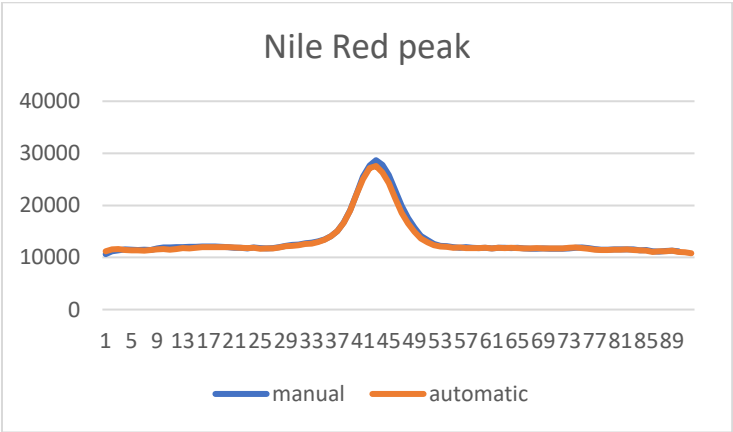


Figure 8. Fluorescence along a single cell length found manually (blue) and automatically (orange).

When comparing the data gathered using the automatic and manual method, the two datasets are very similar every time. One of these comparisons is shown in figure 8. This shows that the way the data is collected is not the cause of the difference between the results from the automatic data collection method and the results found manually.

4. Colocalization of fluorescence peaks

Because of the ChainTracer tool measuring the fluorescence along the entire length of the cell it is easy to pin point the relative location of the septal peak according to the length of the cell body. Comparing HADA, FM464 and Nile Red fluorescence peaks location can give us information about the relative location of peptidoglycan synthesis and septal membrane formation. The mutated strain might hinder colocalization of these two processes as FloA and FloT proteins play a role in peptidoglycan synthesis localization (Zielińska et al., 2020). Using Chaintracer, the relative position of HADA, FM464 and Nile Red fluorescence peaks were found. The distance between HADA and NR fluorescence signal peaks relative to cell length, and the distance between HADA and FM464 fluorescence signal peaks relative to cell length were measured (Figure 9a and b, respectively). This was done for WT and $\Delta floAT$ strains.

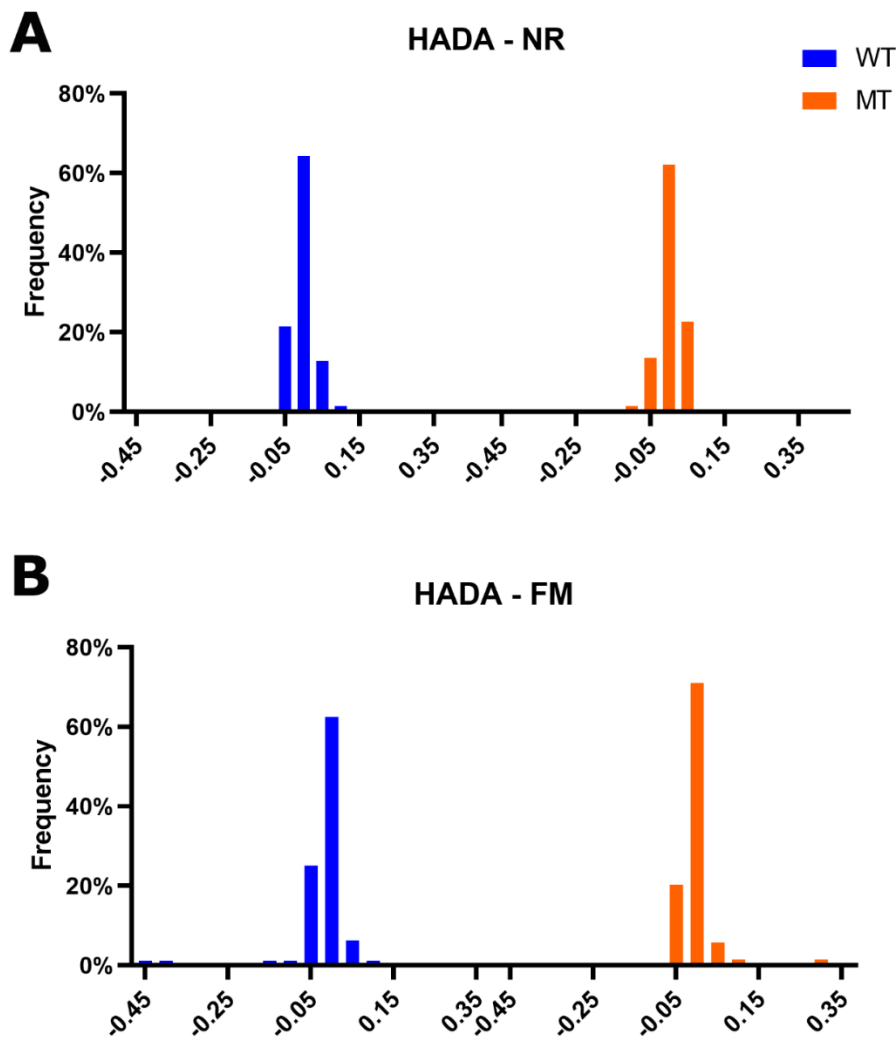


Figure 9. Frequency distribution of the fluorescence peak position of fluorophores relative to cell length. As closer the values are from zero, closer to cell centre the fluorescence peaks were identify.

As the frequency distribution shows, when comparing the fluorescence peaks for HADA and Nile Red, and HADA and FM 464 they are localized in close proximity (Figure 8) The distance between HADA and Nile Red fluorescence peaks are 0 or very close to 0 in the majority of both cell types (In 97.1% of wildtype cells the distance between both peaks was less than 5% of cell length. In 98.4% of $\Delta floAT$ cells the distance between the peaks was less than 5% of cell length. The same can be said for the comparison between HADA peaks and FM peaks (In 97.5% of wildtype cells the distance between both peaks was less than 5% of cell length. In 97.1% of $\Delta floAT$ cells the distance between the peaks was less than 5% of cell length). This suggests that peptidoglycan synthesis is taking place in the same place along the cell length as the septum is being formed for both bacteria strains analysed.

Conclusion

The data collected using ChainTracer matches up with the data collected by hand (Figure 8). This shows that automating the collection of fluorescence data is a reliable way of improving analysis speed of cellular fluorescence profiles. The method present in this work is a reliable and fast way to find fluorescence profiles along the length and width of cells automatically. Therefore this is a useful tool for researchers analysing fluorescence profiles of cells.

The data collected in this study seems to conflict with the data collected in the study done previously by our group (Zielińska et al., 2020). This study shows that the difference in fluorescence peak intensity between wildtype and $\Delta floAT$ strains is not significant for FM or Nile Red dyes.

The difference in results from the manually collected data and the automatic one could be explained by a different approach in data collection. The automation of background fluorescence collection might have played a role in the different results. This is not very likely as it was shown that the automatically collected background fluorescence was nearly always very close to the manually collected background fluorescence value. What might also have influenced the results is that when septa are selected manually, clearly visible septa might be selected more readily than less visible septa, creating a bias in the measurement process. This would cause the manually collected fluorescence peaks to display higher values. This could explain why the fluorescence peak values found automatically are lower than the ones found manually. The difference between $\Delta floAT$ and wild-type fluorescence peak intensity was smaller for the automatically collected data than for the manually collected data. This result might also have been influenced by the possibility that more visible septa were picked in the manual analysis.

The tool developed for measuring fluorescence profiles along the cell width (Figure 2) is useful when data is collected for cells containing multiple septa but information about one of these septa is needed. The developed tool also measures fluorescence outside the cell allowing for background fluorescence measurements. The guidelines of this tool, and how to use it is further described in the appendix of this work "Manual for automatic ChainTracer".

References

Syvertsson, S., Vischer, N.O., Gao, Y. and Hamoen, L.W., 2016. When Phase Contrast Fails: ChainTracer and NucTracer, Two ImageJ methods for semi-automated single cell analysis using membrane or DNA staining. *PLoS one*, 11(3), p.e0151267.

Ducret, A., Quardokus, E.M. and Brun, Y.V., 2016. MicrobeJ, a tool for high throughput bacterial cell detection and quantitative analysis. *Nature microbiology*, 1(7), pp.1-7.

Typas, A., Banzhaf, M., Gross, C.A. and Vollmer, W., 2012. From the regulation of peptidoglycan synthesis to bacterial growth and morphology. *Nature Reviews Microbiology*, 10(2), pp.123-136.

Zhao, H., Patel, V., Helmann, J.D. and Dörr, T., 2017. Don't let sleeping dogmas lie: new views of peptidoglycan synthesis and its regulation. *Molecular microbiology*, 106(6), pp.847-860.

García-Fernández, E., Koch, G., Wagner, R.M., Fekete, A., Stengel, S.T., Schneider, J., Mielich-Süss, B., Geibel, S., Markert, S.M., Stigloher, C. and Lopez, D., 2017. Membrane microdomain disassembly inhibits MRSA antibiotic resistance. *Cell*, 171(6), pp.1354-1367.

Zielińska, A., Savietto, A., de Sousa Borges, A., Martinez, D., Berbon, M., Roelofsen, J.R., Hartman, A.M., de Boer, R., Van der Klei, I.J., Hirsch, A.K. and Habenstein, B., 2020. Flotillin-mediated membrane fluidity controls peptidoglycan synthesis and MreB movement. *eLife*, 9, p.e57179.

Stylianidou, S., Brennan, C., Nissen, S.B., Kuwada, N.J. and Wiggins, P.A., 2016. SuperSegger: robust image segmentation, analysis and lineage tracking of bacterial cells. *Molecular microbiology*, 102(4), pp.690-700.

